

Macroporous Silicon Oxycarbide Fibers with Luffa-like Superhydrophobic Shells

Ping Lu¹, Qing Huang^{2,*}, Baodan Liu³, Yoshio Bando³, You-Lo Hsieh¹, Amiya K. Mukherjee^{2,*}

1, Fiber and Polymer Science, University of California, Davis, CA 95616, USA; 2, Department of Chemical Engineering & Materials Science, University of California, Davis, CA 95618, USA; 3, International Center for Materials Nanoarchitectonics (MANA), National Institute for Material Science, Tsukuba, 305-0044, Japan.

Synthesis procedure

Electrospinning process: Pre-ceramic precursor polyureasilazane (PUS) and poly(methyl methacrylate) (PMMA) (Mw ~120,000, Aldrich) mixed at a 1/3 weight ratio in acetone and vigorously stirred for 24 h in a close vial. The PUS/PMMA solution was loaded into a 20 ml syringe (National Scientific) fitted with a 23 gauge inner diameter metal needle (BD Medical Franklin Lakes, NJ), fed at a rate of 20 mL/h by a syringe pump (KDS 200, KD Scientific, USA) and electrospun by applying a 15 kV voltage with a DC power supply (ES 30-0.1 P, Gamma High Voltage Research Inc., Ormond Beach, FL) to the needle. The charged jet of solution was sprayed into fine fibers that were collected at 24 °C and 38% relative humidity on a perpendicularly-standing aluminum plate (30 cm × 30 cm) placed 25 cm from the needle. An as-electrospun PUS/PMMA fibrous mat was then dried at ambient temperature under vacuum for 48 h for the subsequent experiments. PMMA was also electrospun into fibers from a 15 wt% acetone solution without PUS, using the same synthesis procedure for comparison.

Calcination: PUS/PMMA fibers were calcined in a two-step process. The samples were first heated in nitrogen atmosphere at a fast heating rate of 10 °C/min to 120 °C and then incubated for 60 min to stabilize the fiber structures. The temperature was then slowly increased, at 5 °C/min to 500 °C and was held at 500 °C for 2 h, to completely remove PMMA.

Characterization

Microstructures: The morphologies of products were examined by a scanning electron microscope (SEM) (XL 30-SFEG, FEI/Philips, USA) after gold coating (Bio-Rad SEM coating system). A transmission electron microscope (TEM, Philips CM-12) was used to observe the cross-section and the shell-core structures of calcined fibers. The fibers were first embedded in a thermal curable resin, and then solidified resin was cut by a

microtome to obtain thin sections for TEM observation. The element composition and their distribution were measured using an energy filtering electron microscope equipped with OMEGA-type energy filter and operated at an accelerating voltage of 300kV. The special resolution is 0.5 nm.

Physical and chemical structures: The phase structures in the products were determined by X-ray powder diffraction (XRD) using Cu K α radiation on a Scintag XDS 2000 powder diffractometer. The chemical structures were determined by ^{29}Si solid state nuclear magnetic resonance (NMR) technique. An ^{29}Si solid state MAS NMR experiment was carried out with a Bruker 500 AVANCE spectrometer equipped with an 11.74 T magnet. A 7 mm Bruker probe was used. The fiber sample was loaded in a 7mm zirconia rotor at a 5KHz spinning speed. Direct polarization pulse sequence was used with a 60 degree tip angle and 5 minute recycle delay. The chemical shift was externally referenced to tetramethylsilane (TMS). The FTIR spectra spanning from 4000 to 500 cm^{-1} was obtained at a resolution of 4 cm^{-1} by a Nicolet 6700 spectrometer (Thermo Fisher Scientific, USA). The thermal behaviors of the PMMA fibers, PUS polymer and as-spun composite fibers were also measured under N_2 using a thermogravimetric analyser (TGA-50, Shimadzu, Japan).

Pore structure characterization: The surface areas, pore sizes and pore size distribution of the fibers including PMMA fibers, as-spun composite fibers and as-calcined composite fibers, were measured by N_2 adsorption-desorption isotherms at 77 K or the Brunauer-Emmett-Teller (BET) method using a Surface Area and Porosity Analyzer (ASAP 2020, Micromeritics, USA).

Oil absorption measurement: The as-calcined PUS/PMMA membrane was cut into small pieces at about 2 mg apiece. The exact mass of the sample was measured and recorded as W_i . The sample was then immersed in certain oil for 10 min. The wetted sample was dabbed dry, hung in air for 10 s to reach equilibrium and weighted to obtain W_f . The oil absorption capacity was calculated from mass gain using the following equation:

$$\text{Weight gain (\%)} = (W_f - W_i)/W_i \times 100$$

The dynamic oil absorption of as-calcined fiber mats was measured by a liquid tensiometer (K14, KRÜSS, USA).

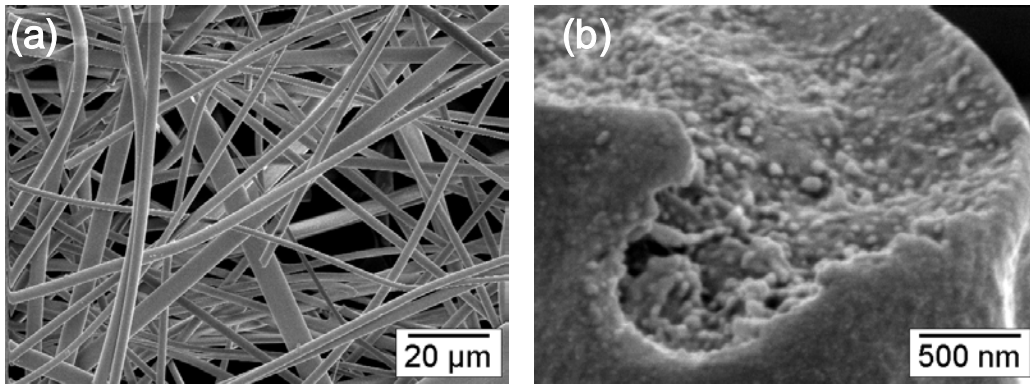


Figure S1. SEM images of as-spun PUS/PMMA composite fibers (a) and cross section of one fiber.

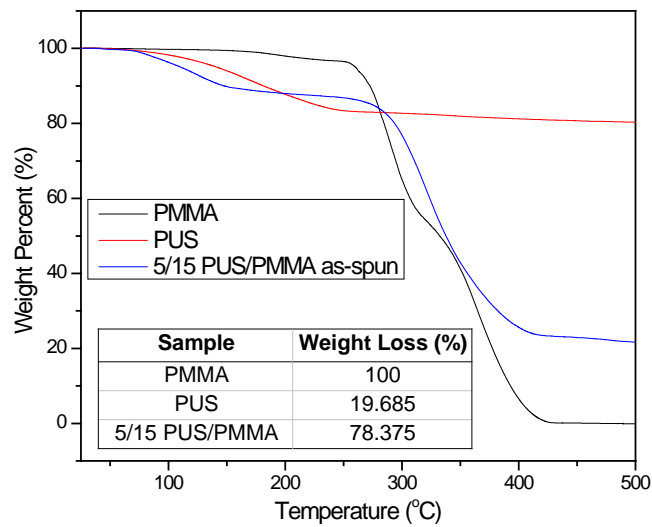


Figure S2. Thermogravimetric analysis showing the weight losses of the PUS precursor, imbedding PMMA polymer and PUS/PMMA fibers. Based on these data, PMMA polymer was completely burned out in the as-calcined fibers.

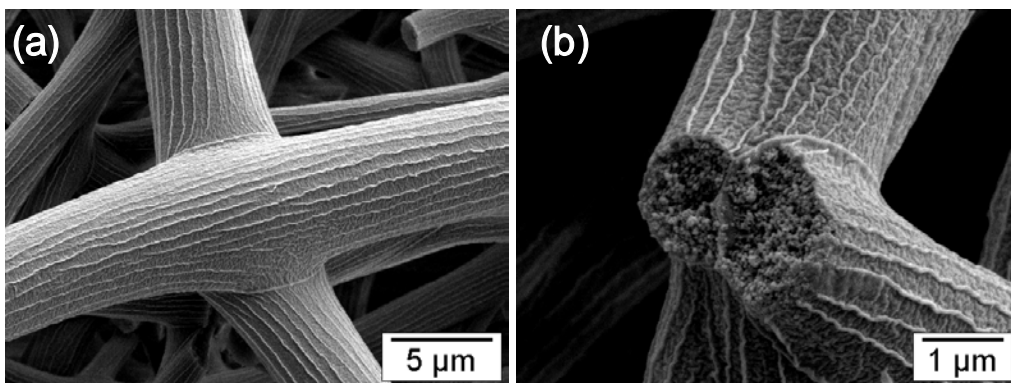


Figure S3. SEM images (a) and (b) showing the fusion of adjacent fibers that formed a three dimensionally macroporous fiber network.

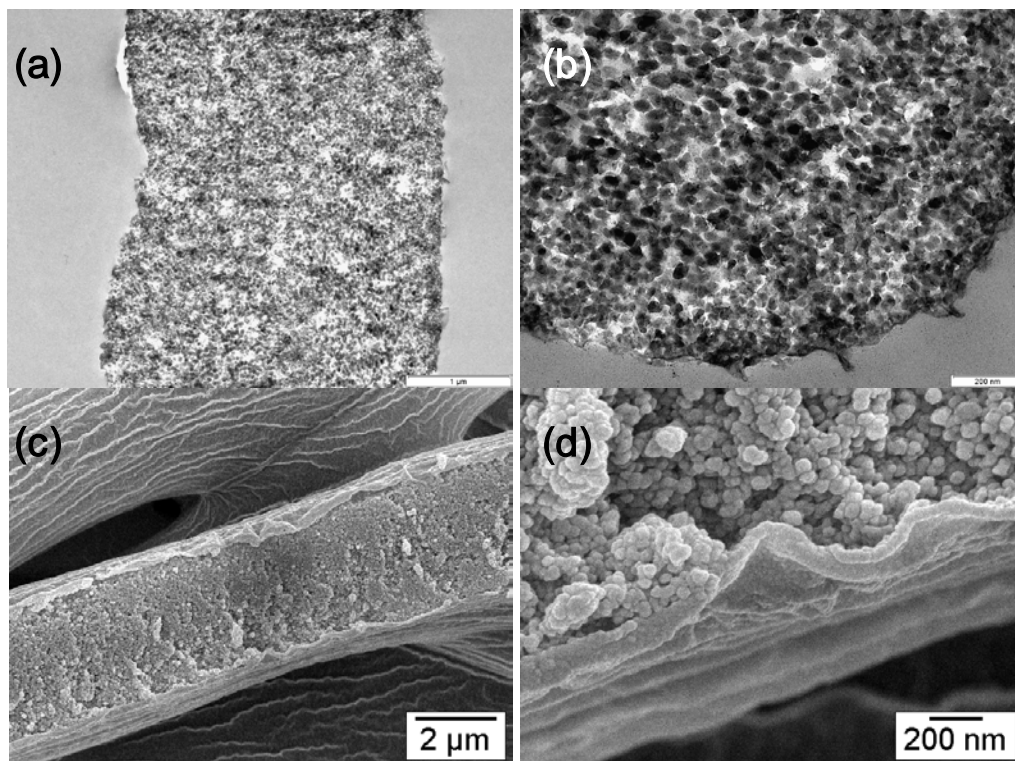


Figure S4. TEM images of sliced fibers along the axial (a) and radial directions (b) clearly showing nanoparticles capsulated by a layer of shell and nano-pores in the fibers. SEM images also present the same microstructures (c and d). The shell thickness is about 50 nm as that of the diameter of nanoparticles.

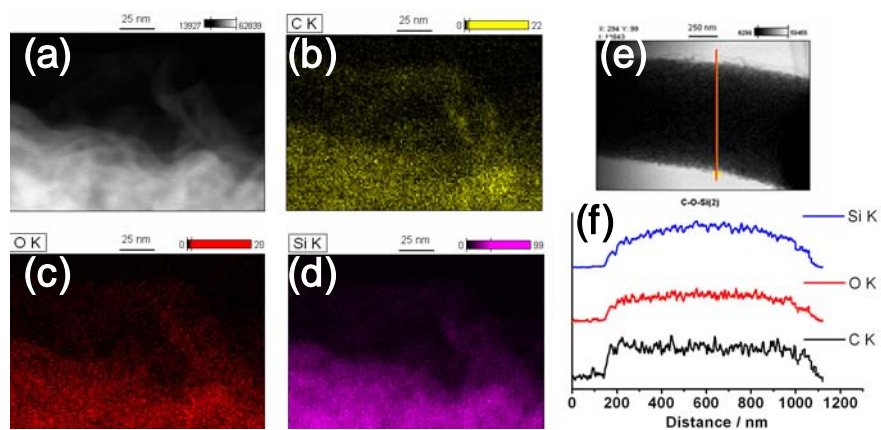


Figure S5. Elemental mapping of an as-calcined fiber (a) indicating the distribution of C (b), O (c), Si (d) elements. Obviously, both shell and core regions contain these elements. A line-scan spectrum (f) of a fiber (e) showing the variation of signal intensity along the radial direction.

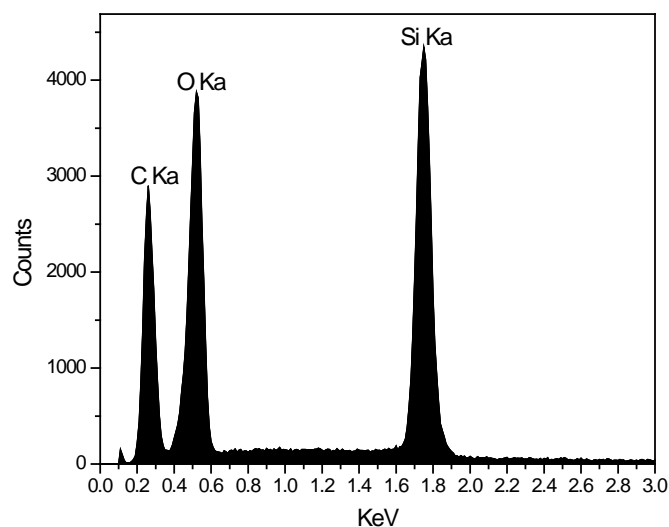


Figure S6. Energy-dispersive X-ray spectrum of as-calcined fibers.

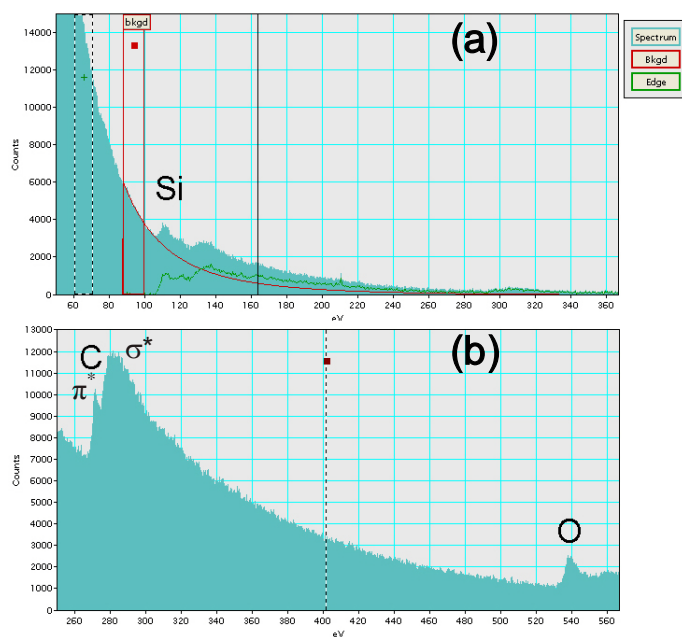


Figure S7. EELS spectra of an as-calcined fiber showing the presence of Si, C, and O elements. The peak at 113 eV in the Si plot indicates the amorphous state of silicon composite in resultant silicon oxycarbide fibers (a). Nitrogen signal is absent as indicated by in Figure (b). The first peak (left one) and second peak (right one) in the graphite plot are due to absorption by π^* bond and σ^* bond of carbon atom, respectively.

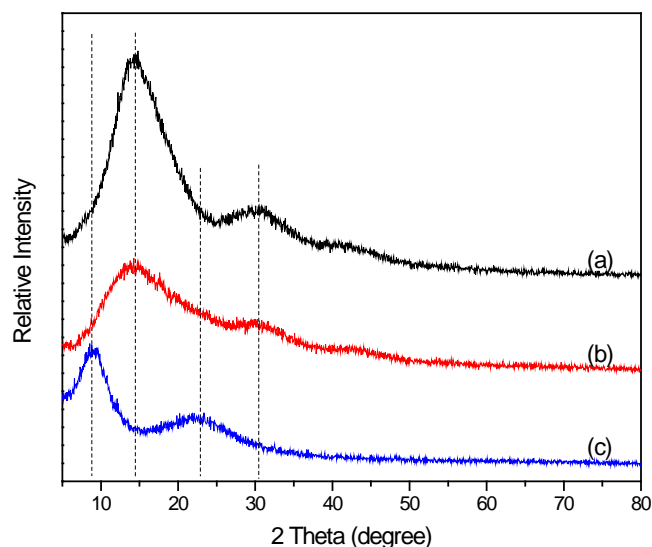


Figure S8. XRD patterns of (a) as-spun PMMA fibers, (b) as-spun PUS/PMMA fibers, and (c) as-calcined PUS/PMMA fibers. No crystalline phase exists in the products. The broadened diffraction peak is the typical semi-crystalline behavior of polymers.

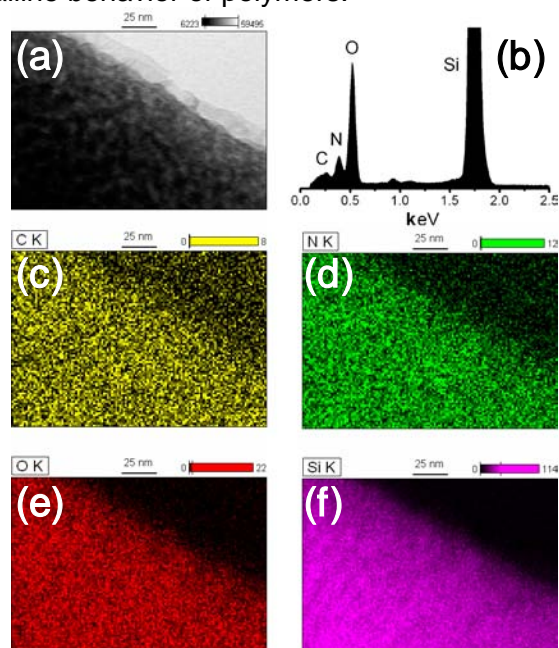


Figure S9. Scanning transmission electron microscopy (STEM) image showing the morphology of an ammonia-treated SiOC fiber (a). A layer of shell with thickness of 20 nm and porous core region are visible in the product, indicating the microstructure was preserved after high-temperature annealing. Obviously, nitrogen substituted carbon in the as-calcined fibers as shown in corresponding EDS spectrum (b), the relative intensity of carbon reduced substantially as compared to the original one (Figure S6). Elemental mapping images of C (c), N (d), O (e) and Si (f) reveal the distribution of these elements in a fiber. Obviously, N substituted C throughout the whole fiber (d).

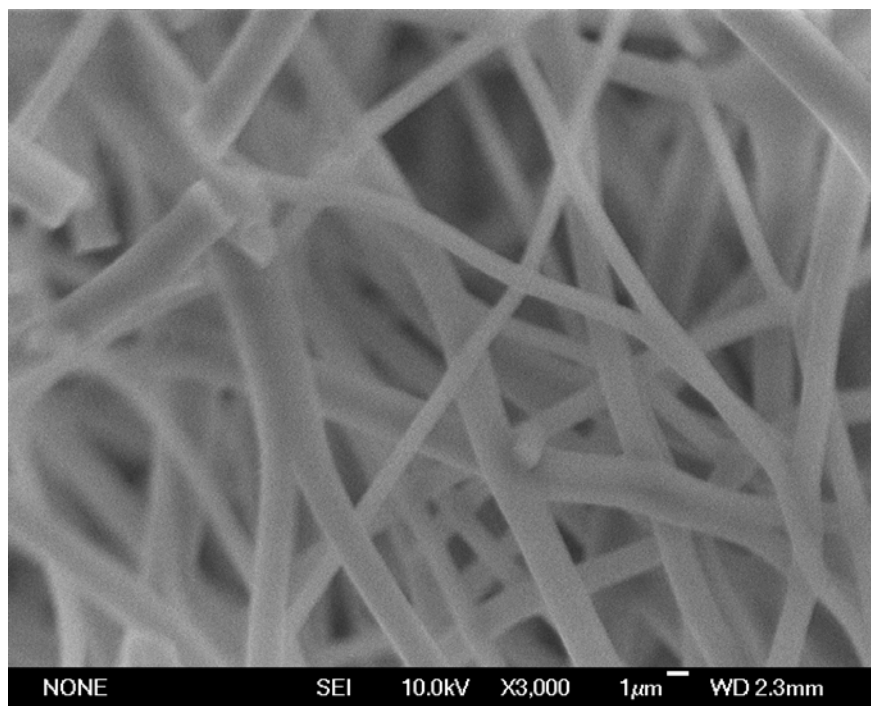


Figure S10. SEM image of N-substituted fibers. The substitution of N for C in fibers leads to decrease in electrical conductivity, therefore, some charges gathered on the surface of fibers in the SEM mode.

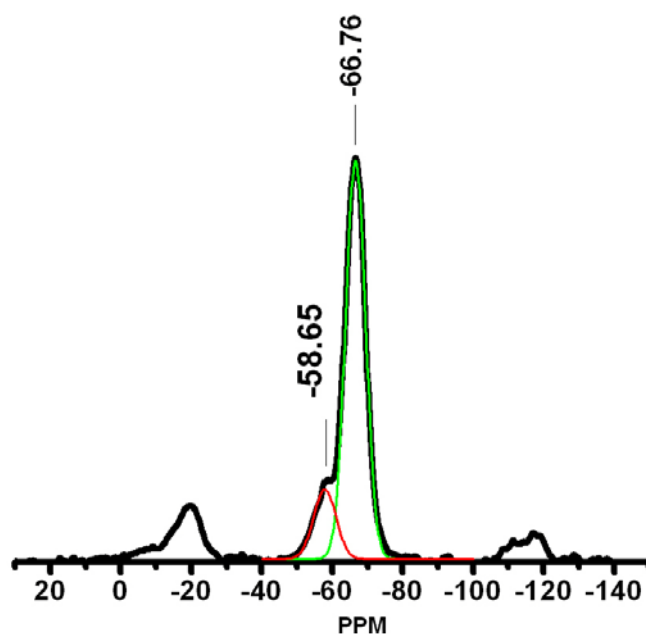


Figure S11. ^{29}Si NMR spectrum of as-calcined fibers. Two characteristic peaks corresponding to $(\text{SiO}_3)\text{SiCH}_3$ (-66.7 ppm) and $(\text{SiO}_2)\text{SiCH}_3\text{OH}$ (-58.6 ppm) are resolved by gauss' function. The small peaks at -20 and -120 ppm are spinning side bands not related to the fiber structure.

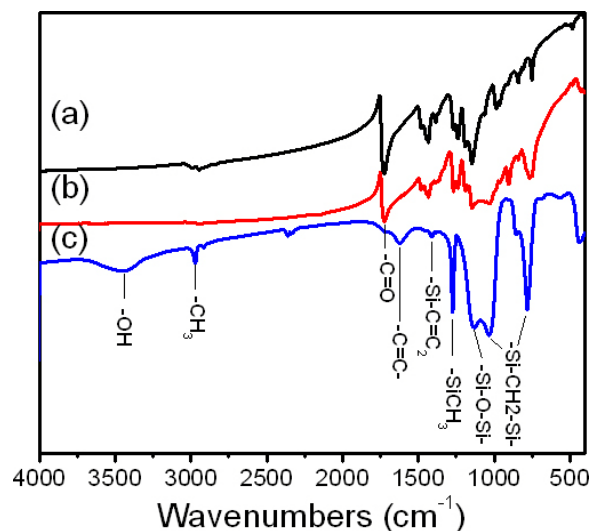


Figure S12. FTIR of (a) as-spun PMMA fibers, (b) as-spun PUS/PMMA fibers and (c) as-calcined SiOC fibers. Some chemical groups are marked at their corresponding vibration peaks. The disappearance of $-C=O$ bond means the burnout of PMMA in the as-calcined fibers, while the cross-linking of PUS is shown by absorption characteristic of vibration bonds, such as $-Si-C=C_2$, $-Si-O-Si-$, $-Si-CH_2-Si-$, and $-Si-CH_4$.

Table 1. BET surface areas and pores of as-spun PMMA fibers, as-spun PUS/PMMA fibers and as-calcined PUS/PMMA fibers

	BET surface area (m ² /g)	BJH adsorption cumulative surface area of pores (1.7-300 nm) (m ² /g)	BJH adsorption cumulative volume of pores (1.7-300 nm) (cm ³ /g)	BJH adsorption average pore width (4V/A) (nm)
PMMA*	2.159±0.032	1.944±0.127	0.00511±0.00024	10.51±0.23
PUS/PMMA**	1.495±0.014	1.618±0.031	0.00345±0.00023	8.52±0.40
PUS/PMMA***	391.772±0.408	190.850±0.142	0.56384±0.00565	11.82±0.13

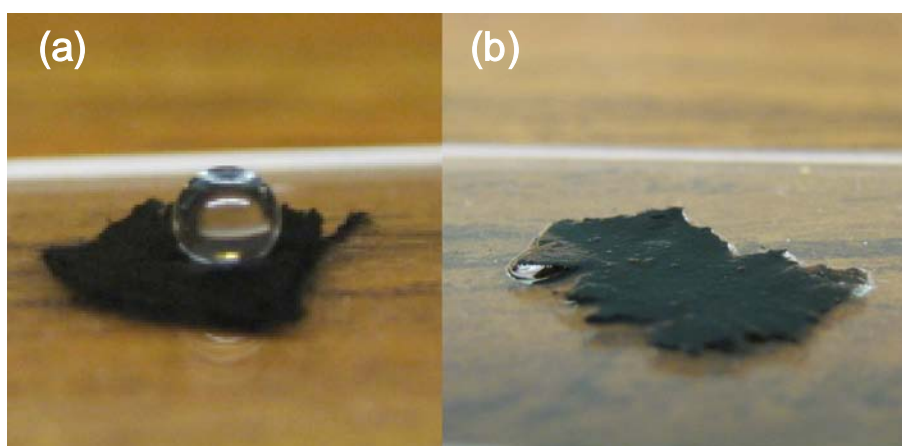


Figure S13. Photos showing a water drop (a) and absorption of octane solvent (b) on the as-calcined fiber mats.

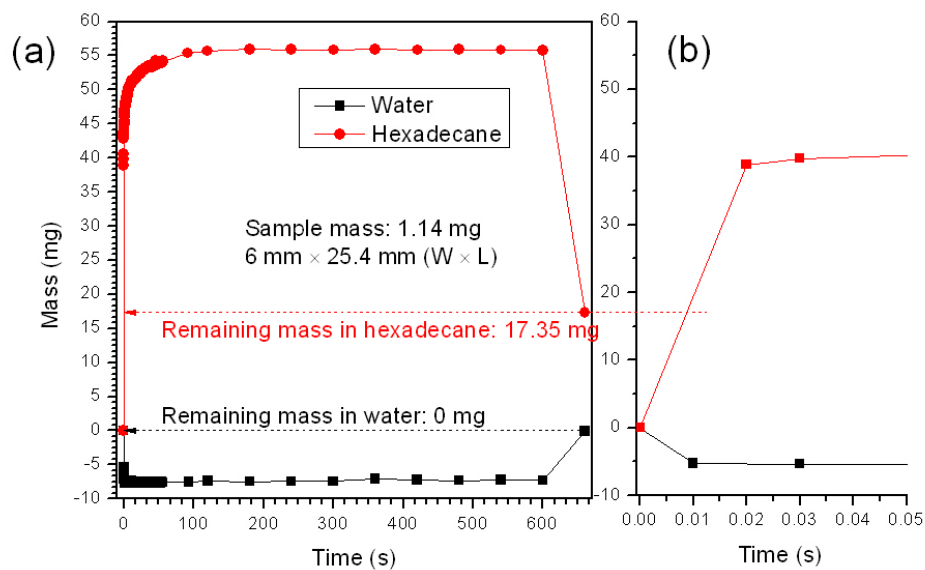


Figure S14. Dynamic absorption curves for as-calcined fiber mat. As soon as fibers (1.14 mg) contacted hexadecane solution, the organic solvent was immediately absorbed, and the weight gain of fiber mat is up to 56.82 mg, 50 times of original fiber weight (a). When fiber mat retrieved from solution at 600 s, the weight of hexadecane capsulated in fibers is still very large (17.35 mg), meaning the uptake capacity for hexadecane is 15.2 times by weight. In the case of contacting water solution, a compelling force loaded on the fibers due to their superhydrophobic surface. Since no water molecule has been attached on fibers, weight gained returned to zero when fiber mat was retrieved from water. Another feature obtained from this measurement is that solvent absorption is instantaneous (b), all fibers were filled by hexadecane in a short time that beyond detection limit of the apparatus (less than 0.02s).